

Wave energy absorption by a floating air-filled bag

Adi Kurniawan, Deborah Greaves, Martyn Hann
Plymouth University, Plymouth PL4 8AA, UK

John Chaplin, Francis Farley
University of Southampton, Southampton SO17 1BJ, UK
E-mail: adi.kurniawan@plymouth.ac.uk

Highlights

- Measurements of capture widths and motions of a floating air-filled bag subjected to regular incident waves and equipped with a power take-off.

1 Introduction

We study a wave energy device featuring a deformable flexible bag which encloses a volume of air. As the device heaves under wave action, expansion and contraction of the bag result in an air flow into and out of a separate volume via an air turbine (fig. 1(a)). Although similar to the Lancaster flexible bag device of the 1970s [5] in its use of deformable flexible structures, the main motivation behind the present device was the fact that, being compressible, the device could have a resonance period longer than a rigid device of the same size, resulting in a potential cost reduction [4].

At the last workshop, we presented a study of the device when forced to heave in still water by means of an oscillating pump [2]. The measured heave response was compared with predictions of a linear frequency-domain model which used a finite difference approach to model the bag deformation. The predictions agreed reasonably well with the measurements, and the lengthening of the heave resonance period of the device compared to that of a rigid device of equal dimensions was confirmed. Further, we found that as the bag was slowly deflated from almost full, the pressure in the bag first decreased, reaching a minimum before then increasing as the device continued to descend. Thus, for a given pressure, there are two possible bag shapes having the same pressure. An example is shown in fig. 2(a & b).

In the present paper, the same device is subjected to regular incident waves and absorbs energy from the waves. The measured motion and power absorption characteristics of the device under various controlled conditions are presented and discussed. The capture width of the device is shown to peak at a period over 25% longer than the peak period of a rigid body of the same dimensions, while the peak absorbed power and the relative bandwidth are similar to those of the rigid body.

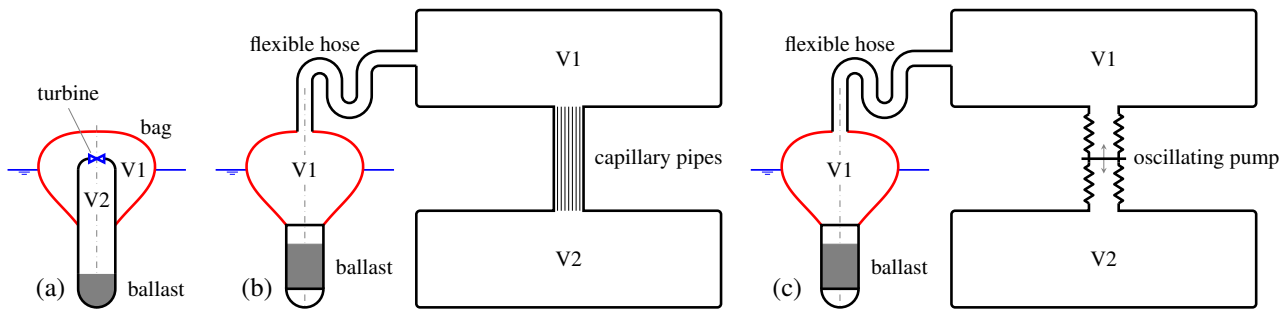


Figure 1: Schematics of (a) the full-scale device and the small-scale models in (b) the incident wave tests and (c) the forced heaving tests.

2 Model test setup

Small-scale tests of the device were conducted in the 35 m × 15.5 m wave basin at Plymouth University. The water depth was 3 m. The setup was similar to that of the forced heaving tests [2], the main difference being that the pump was replaced with an assembly of capillary pipes, described in [3], to represent a linear power take off (PTO). The PTO damping could be varied by opening and closing a number of pipes in the capillary pipe assembly. In addition, the construction of the bag was slightly different. Previously, the bag was made by joining together identical petals of fabric, with tendons welded along the seam. The present bag was made from two circular fabric discs welded together along the perimeters, and the tendons were not welded onto the fabric, but ran through guides attached to it (see fig. 2). The present bag was also smaller: its tendon length was 1 m as opposed to 1.5 m for the previous one, and the bag displacement was 100 kg as opposed to 340 kg. Both bags have the same number of tendons, i.e. 16, and the fabrics were both made of unreinforced polyurethane film. Fig. 1 shows the setup of the present tests compared to the previous tests.

In order for the deformation of the bag to scale as $1/s$ at model scale, any air volume has to be scaled according to

$$V_m = \frac{p_{\text{atm}}s + p_{10}}{p_{\text{atm}} + p_{10}} \frac{V}{s^3}, \quad (1)$$

where V_m and V are the model-scale and full-scale air volumes, respectively, p_{atm} is the atmospheric pressure, and p_{10} is the mean pressure in the system (minus the atmospheric pressure). Equation (1) may be represented as fig. 3. If $p_{10} = 0$, such as in an oscillating water column device, the required air volume at model scale is V/s^2 . For $p_{10} > 0$, as in our case, the required model-scale air volume is less than V/s^2 , but still greater than V/s^3 . This means that, at model scale, large enough air volumes had to be added either side of the PTO, as shown in fig. 1. We used three air tanks, each with a capacity of 1100 litres, in our tests: one tank on the V1 side, and two tanks on the V2 side. The number of connected air tanks could be varied by means of valves, so that any of these four combinations of V1 + V2 tanks could be tested: 0 + 1, 0 + 2, 1 + 1, or 1 + 2. If we adopt $s = 24$ for our model, the full-scale V1 and V2 volumes corresponding to the number of V1 and V2 tanks in use and for an equilibrium bag shape as shown in fig. 2(c) can be calculated based on (1). These are listed in table 1. To allow free movement of the device, a flexible hose was used to connect the bag to the rest of the system.

The displacements of the top of the bag and of the ballast cylinder were recorded using infrared cameras. In addition, two video cameras recorded the motions of the device from the side: one above water and the other under water. Two pressure transducers, one on each side of the PTO, were used to record the pressures either side of the PTO. To investigate the effects of restraining or unrestraining the device in pitch, horizontal parallel lines were used to moor the device as shown in fig. 4. The nominal incident wave amplitude in the regular wave tests was always 2 cm.

3 Results and discussions

All the following results are for the device with a mean pressure of 37 cm and a bag shape shown in fig. 2(c).

Only the first harmonics of the recorded oscillations were used in the analysis. To obtain the first harmonics, the recorded time histories of the free-surface elevation, pressures, and displacements of the device were first high-pass filtered and then a harmonic function in the form of $a \cos(\omega t + \alpha)$, where ω is the wave frequency, was fitted in the least-squares sense to a selected portion (about 10-second duration) of each of the filtered signals.

The measured absorbed power of the device was obtained from the recorded pressures at either side of the PTO and the known damping of the PTO, which could be determined theoretically from Poiseuille's equation for laminar flow in smooth pipes. To compute the absorbed power and heave displacement of a rigid body with dimensions equal to the device, WAMIT [6] was used to obtain the hydrodynamic coefficients. The mass of the body was 143 kg and a constant PTO damping of 90 kg/s was used.

Effects of PTO damping and size of V2. From the data (not shown), we observe that as more PTO tubes are open, there is in general a slight increase in the absorbed power but little effects on the device motions. Having more PTO tubes open, i.e. decreasing the PTO damping, reduces the amplitude of p_1 , i.e. the pressure in V1, and increases the amplitude of p_2 , i.e. the pressure in V2. This is reasonable, as with more PTO tubes open, the two volumes become more like a single volume and the difference between the two pressures gets smaller. With larger V2, the amplitudes of p_1 and the heave response were almost unaffected, while the capture width is slightly increased, but the most noticeable effect is the decrease of pressure amplitudes in V2. In fig. 5, the ratio of p_1 to p_2 amplitudes as well as the phase difference between p_1 and p_2 are plotted alongside predictions based on the linearised adiabatic relation, which shows that the two quantities are the modulus and phase of

$$\frac{p_1}{p_2} = 1 + i \left(\frac{2\pi V_{20} R_{\text{PTO}}}{\gamma p_0 T} \right), \quad (2)$$

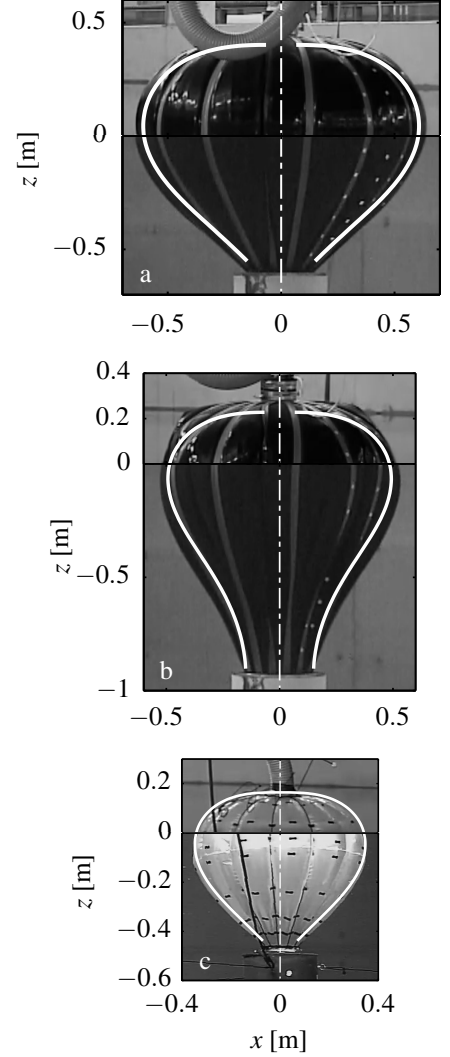


Figure 2: Static shapes for (a & b) 1.5-m tendon bag, pressure = 0.4 m of water, and (c) 1-m tendon bag, pressure = 0.37 m of water. The calculated shapes are obtained using the method described in [1].

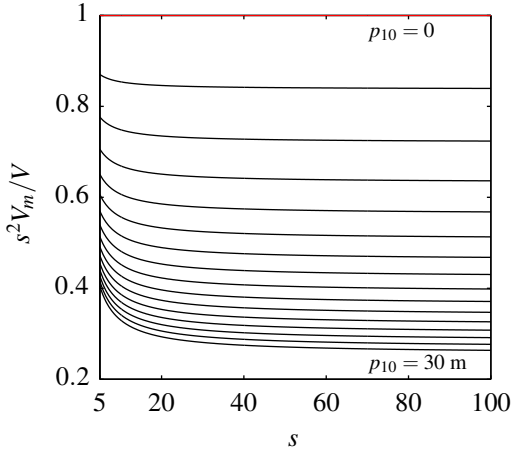


Figure 3: Ratio of model-scale air volume to full-scale air volume / s^2 . Lines correspond to various full-scale pressures from 0 to 30 m of water, in 2 m increment.

where V_{20} is the volume of V2, R_{PTO} is the PTO damping, p_0 is the mean pressure in the system, and $\gamma = 1.4$. The theory appears to agree well with the measurements. For the same mean pressure p_0 , as $V_{20}R_{PTO}$ gets smaller, the pressures in the two volumes become more similar both in amplitude and phase.

Effects of size of V1. Fig. 6 shows that increasing the size of V1 has the effect of lengthening the device resonance period. With no V1 tanks, the capture width has a peak period of about 1.6 s, or 7.8 s at full scale. With one V1 tank, the peak period is lengthened further to about 1.8 s, or 8.8 s at full scale. The latter is over 25% longer than the peak period of a rigid body of equal dimensions, which is 6.9 s at full scale. Note that the full-scale volume of V1 in the case with one V1 tank is still smaller than the full-scale volume of the bag (see table 1). Also plotted in fig. 6 are the peak heave response periods of the bag when forced to heave by means of an oscillating pump, calculated using the method described in [2]. These are shown to be close to the peak periods of the capture width.

The peak capture widths relative to the waterplane diameter are 0.58 with no V1 tanks and 0.51 with one V1 tank. Although these are lower than that of the rigid body, the peak mean absorbed power of the device for both cases is in fact comparable to that of the rigid body, since the incident wave power is proportional to the wave period. It is also observed that the relative bandwidths for the two cases are similar to that of the rigid body. The Q factor, i.e. the inverse of the relative bandwidth, can be shown to be about 4.

We may finally note from fig. 6 that the peak periods of the heave RAO are about 0.1–0.2 s longer, or 0.5–1.0 s longer at full scale, than the peak periods of the capture width or the pressure amplitudes. This is because the response is damped, and since the capture width is inversely proportional to the cube of the wave period, the effect of damping on the capture width is not as great as that on the RAO.

Effects of moorings. Allowing the device to pitch is found to decrease the absorbed power, the pressure amplitudes, and the heave response of the bag (see fig. 7), but the effects seem to be small. This decrease is likely due to some nonlinear coupling between heave and pitch. When the device pitches more, it is found to heave less, and this leads to a decrease in pressure amplitudes in the bag. With the same PTO damping, this in turn results in a decrease in the absorbed power.

V1 tanks	full-scale V1 volume [m ³]	V2 tanks	full-scale V2 volume [m ³]
0	200	1	1200
1	1300	2	2300

Table 1: Full-scale V1 and V2 volumes for $s = 24$ and a model-scale pressure of 37 cm of water. The full-scale bag volume is 2000 m³.

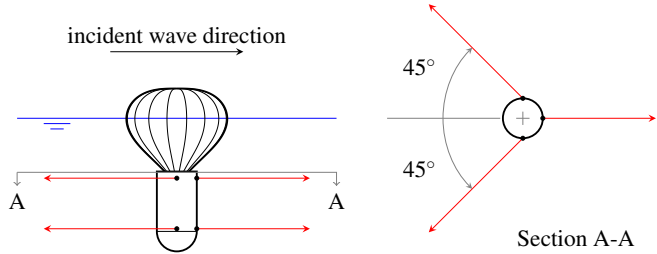


Figure 4: Configuration of the mooring lines.

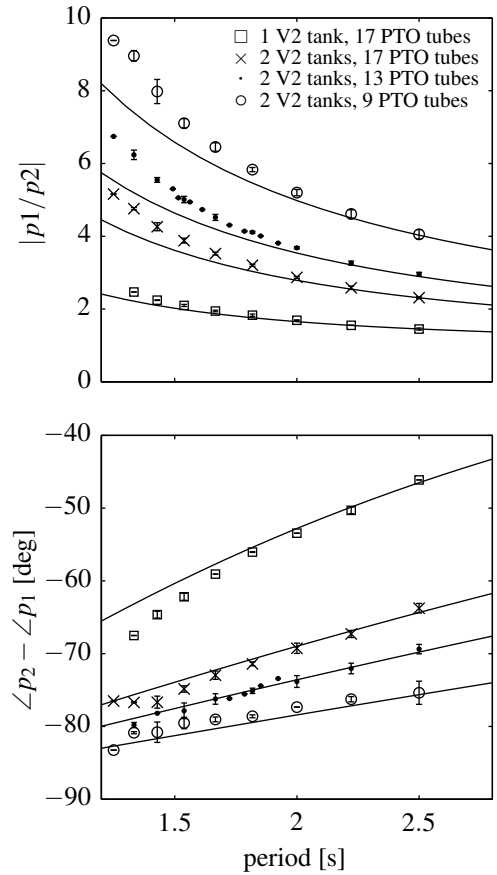


Figure 5: Amplitude ratio and phase difference of pressures across the PTO, for different V2 sizes and PTO damping. Lines are numerical predictions.

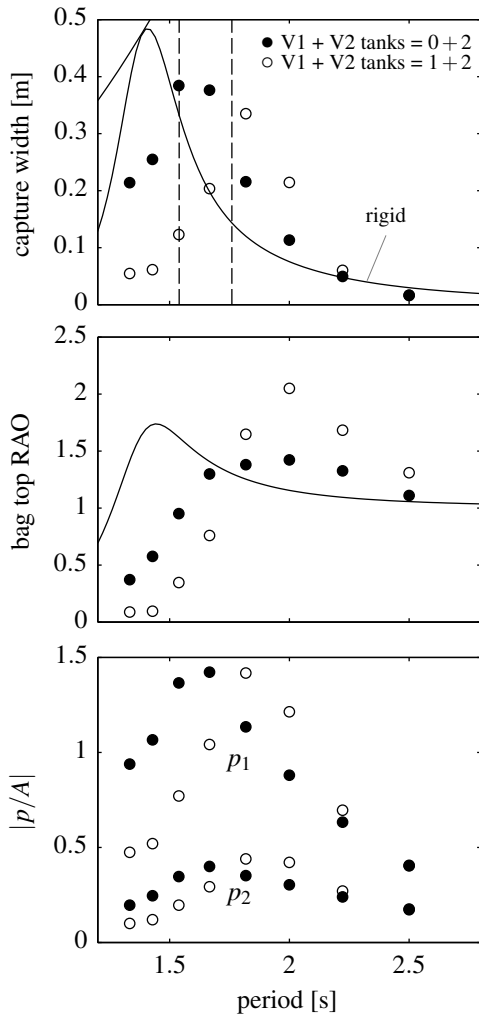


Figure 6: Capture widths, heave RAOs of the top of the bag, and normalised pressure amplitudes for different sizes of V1 and with 17 PTO tubes open. Calculated heave peak periods of the bag for the forced heaving case are shown by dashed lines.

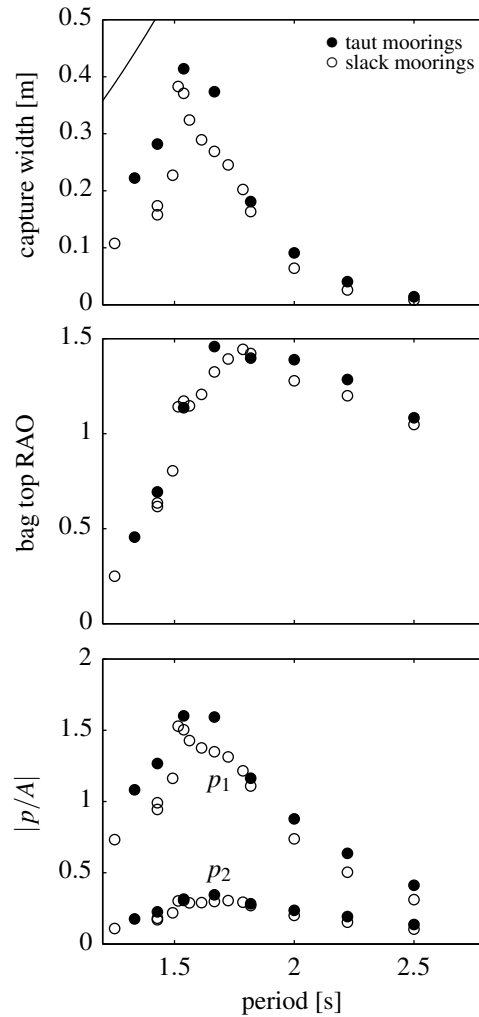


Figure 7: Capture widths, heave RAOs of the top of the bag, and normalised pressure amplitudes with the moorings taut and slack, for V1 + V2 tanks = 0 + 2 and with 13 PTO tubes open.

Acknowledgement

This work is supported by the EPSRC SuperGen Marine Energy Research Consortium [grant no. EP/K012177/1]. We are grateful to Malcolm Cox of Griffon Hoverwork Ltd for supplying the model test bag and for useful discussions.

References

- [1] Chaplin, J., Farley, F., Greaves, D., Hann, M., Kurniawan, A., and Cox, M. (2015a). Numerical and experimental investigation of wave energy devices with inflated bags. In *Proc. 11th Eur. Wave and Tidal Energy Conf.*, Nantes, France.
- [2] Chaplin, J. R., Farley, F., Kurniawan, A., Greaves, D., and Hann, M. (2015b). Forced heaving motion of a floating air-filled bag. In *Proc. 30th Int. Workshop on Water Waves and Floating Bodies*, Bristol, UK.
- [3] Chaplin, J. R., Heller, V., Farley, F. J. M., Hearn, G. E., and Rainey, R. C. T. (2012). Laboratory testing the Anaconda. *Phil. Trans. R. Soc. A*, 370(1959):403–424.
- [4] Farley, F. J. M. (2011). The free floating clam - a new wave energy converter. In *Proc. 9th Eur. Wave and Tidal Energy Conf.*, Southampton.
- [5] French, M. J. (1979). The search for low cost wave energy and the flexible bag device. In *Proc. 1st Symp. Wave Energy Utilization*, pages 364–377, Gothenburg, Sweden.
- [6] WAMIT (2013). WAMIT, Inc., Chestnut Hill, MA. Version 7.0.